Proximal threats promote enhanced acquisition and persistence of reactive fear-learning circuits

Leonard Faul[a,1], Daniel Stjepanović[a,b,1], Joshua M. Stivers[a], Gregory W. Stewart[a], John L. Graner[a], Rajendra A. Morey[c], and Kevin S. LaBar[a,c,2]

[a]Department of Psychology & Neuroscience, Duke University, Durham, NC 27708; [b]Centre for Youth Substance Abuse Research, The University of Queensland, St Lucia, QLD 4072, Australia; and [c]Department of Psychiatry and Behavioral Sciences, Duke University Medical Center, Durham, NC 27710

Edited by Joseph E. LeDoux, New York University, New York, NY, and approved June 1, 2020 (received for review March 6, 2020)

Physical proximity to a traumatic event increases the severity of accompanying stress symptoms, an effect that is reminiscent of evolutionarily configured fear responses based on threat imminence. Despite being widely adopted as a model system for stress and anxiety disorders, fear-conditioning research has not yet characterized how threat proximity impacts the mechanisms of fear acquisition and extinction in the human brain. We used three-dimensional (3D) virtual reality technology to manipulate the egocentric distance of conspecific threats while healthy adult participants navigated virtual worlds during functional magnetic resonance imaging (fMRI). Consistent with theoretical predictions, proximal threats enhanced fear acquisition by shifting conditioned learning from cognitive to reactive fear circuits in the brain and reducing amygdala–cortical connectivity during both fear acquisition and extinction. With an analysis of representational pattern similarity between the acquisition and extinction phases, we further demonstrate that proximal threats impaired extinction efficacy via persistent multivariate representations of conditioned learning in the cerebellum, which predicted susceptibility to later fear reinstatement. These results show that conditioned threats encountered in close proximity are more resistant to extinction learning and suggest that the canonical neural circuitry typically associated with fear learning requires additional consideration of a more reactive neural fear system to fully account for this effect.

proximity | fear conditioning | virtual reality | representational similarity analysis | cerebellum

Recognizing potential threats is a fundamental survival skill that enables the appropriate selection of defensive behaviors (1, 2). Given the importance of this evolutionarily configured response, researchers have long studied the underlying processes that support the learning of threat associations. These paradigms typically place a conditioned stimulus (CS) in a predictive relationship with an aversive reinforcer, and then test for the persistence of the acquired defensive response when it is no longer reinforced (3). A dynamic neural system supports the acquisition and extinction of threat associations, involving bidirectional connections among prefrontal, medial temporal, and midbrain structures (4). Specifically, the prevailing neural account highlights the importance of the amygdala in receiving sensory information and generating defensive behavior (5), the hippocampus in storing memory representations for fearful contexts (6), and dorsal and ventral portions of the medial prefrontal cortex (mPFC) in facilitating fear expression or suppression, respectively (7). Moreover, while detailing this general shared network supporting conditioned fear learning, researchers have also examined important modulatory factors that expand our understanding of the complex neural architecture underlying the initial acquisition and long-term maintenance of threat associations. For example, such investigations have indicated dissociable roles for the amygdala and hippocampus in cue and context-related fear conditioning, respectively (8), and that fear generalization to perceptually related stimuli engages a similar set of regions initially active during the learning period (9, 10).

The development of neurocognitive models for conditioned fear learning provides a promising means to better understand psychiatric symptoms of threat hypersensitivity and fear persistence, as exemplified by posttraumatic stress disorder (PTSD) (11, 12). However, most fear-conditioning studies rely on brief presentations of images or sounds as conditioned stimuli, a method that is well-suited for the constraints of traditional research settings but difficult to generalize to many real-life traumatic encounters. In recent years, the development of virtual reality (VR) has offered a promising means by which to address this limitation, as it affords a richer experimental manipulation of both threat cues and contexts, and ultimately provides a more salient and ecologically valid experience (13). VR technology is especially powerful for manipulating spatial distance, which significantly contributes to the severity of trauma-related disorders, but has yet to be incorporated into existing fear-conditioning models. Compared to spatially distal events, traumatic events that directly involve the body envelope, such as rape and assault, are most strongly associated with PTSD (14), and a systematic review showed that direct exposure and close proximity to an

Significance

Traditional laboratory-based fear-conditioning approaches are often limited in their generalizability to real-world encounters where threats are dynamic and embedded in contextually rich environments. Moreover, while spatial distance to a threat organizes defensive responses, our understanding of the neurobehavioral mechanisms relating proximity and fear learning is lacking. To address these limitations, we developed a three-dimensional (3D) virtual reality simulation that provides a more ecologically valid examination of how threat proximity influences the learning and memory of fear associations. Our findings highlight that threats invading peripersonal space persist longer in memory and uniquely recruit a reactive neural fear system, which has important clinical implications for understanding how near-body traumatic experiences exacerbate the development of traumatic stress disorders.

Author contributions: D.S., R.A.M., and K.S.L. designed research; L.F., D.S., J.M.S., and G.W.S. performed research; L.F., J.M.S., and J.L.G. analyzed data; and L.F., D.S., J.L.G., R.A.M., and K.S.L. wrote the paper.

The authors declare no competing interest.

This article is a PNAS Direct Submission.

Data deposition: Behavioral and psychophysiological data are available at Open Science Framework (https://osf.io/jm62y/). Unthresholded statistical maps are available at NeuroVault (https://neurovault.org/collections/6221/).

[1]L.F. and D.S. contributed equally to this work.

[2]To whom correspondence may be addressed. Email: klabar@duke.edu.

This article contains supporting information online at https://www.pnas.org/lookup/suppl/doi:10.1073/pnas.2004258117/-/DCSupplemental.

First published June 29, 2020.

event increases the risk of PTSD development and number of associated symptoms (15). Moreover, spatial proximity to a highly traumatic bank robbery has been found to be a risk factor for PTSD diagnosis 1 mo later, and this relationship is mediated by acute stress up to 2 d following the robbery (16). Yet, while such emerging evidence suggests strong long-term modulatory effects of spatial proximity on fear circuitry, no study to our knowledge has directly assessed how proximity to a conditioned threat influences conditioned-learning circuits in the human brain and subsequent reactivity to threat stimuli.

Findings from nonhuman animals suggest that a relationship between proximity and fear learning stems evolutionarily from predator–prey interactions, whereby a prey's behavior shifts from a strategic to a reactionary defensive state based on distance to a predator (17). According to the predatory imminence continuum, this effect can be understood along three primary phases: 1) A preencounter phase that configures behaviors to minimize contact with a potential threat (e.g., adjusting meal patterns), 2) a postencounter phase after predator detection that elicits freezing and avoidance behaviors to increase escape probability, and 3) a circa-strike defensive mode that activates reactionary fight-or-flight mechanisms if contact with a predator is inevitable. Neurobiological investigations have revealed that these shifts in defensive states involve a dynamic interface among neural systems that coordinate motoric behavior and fear expression. For example, dorsolateral regions of the midbrain periaqueductal gray (PAG) interact with forebrain structures, such as the amygdala, to fully engage innate circa-strike reactions (18), while coordinating motor output via connections to the cerebellum, motor cortex, and mPFC (19–22). Amygdala–midbrain–medullary circuitry mediates postencounter freezing behavior (23), while activation patterns between the prelimbic and lateral amygdala track threat imminence when anticipating or reacting to predatory attacks (24).

Despite advancements in understanding how predatory imminence affects rodent behavior, research on the behavioral and neural response to threat proximity in humans is lacking, given methodological challenges with manipulating egocentric spatial proximity in neuroimaging environments. The few studies that have investigated threat imminence in humans commonly use chase-and-capture video games (25–28), whereby participants navigate a two-dimensional (2D) maze while trying to avoid capture by a virtual predator as an operant reinforcer. In such investigations, increased proximity to a predator in 2D space shifts brain activity from the rostral anterior cingulate cortex (ACC) and ventromedial PFC (vmPFC) to phylogenetically older midbrain regions, such as the PAG (25, 26). Moreover, whereas postencounter contexts are associated with activation of forebrain structures, such as the vmPFC, amygdala, and hippocampus, the circa-strike context shows negative connectivity of the midbrain with these regions (26). These neural findings correspond with consistent behavioral demonstrations that increased proximity to threatening stimuli tends to amplify and maintain defensive responses, as measured via skin conductance (29, 30) and startle (31), emphasizing that threat imminence also configures distinct behavioral outcomes in humans.

To help explain these findings, the survival optimization system (SOS) hypothesis posits two core systems that modulate adaptive behavioral responses to threat imminence: 1) A modulatory, cognitive appraisal system that guides defensive behavior, and 2) a learning system that develops internal probabilistic models to optimize strategy selection (1). Importantly, this hierarchical model helps explain why different components of an adaptive fear system are recruited based on threat proximity, resulting in the differential configuration of prediction and prevention strategies that influence future behavior. Validating this proposal, a recent video game study revealed differences in escape decisions when approached with slow- or fast-attacking predators, reflecting temporal proximity (32). Participants were motivated to flee from a virtual predator as late as possible in order to acquire more money, thus requiring consideration of the distance to the threat, the cost of fleeing, and the cost of staying. Qi et al. (32) found faster-attacking predators elicit a reactive fear circuit comprising the midbrain and midcingulate cortex (MCC) that facilitates rapid escape decisions, whereas slower-attacking predators resulted in activation of fear circuitry implicated in cognitive appraisals and associative learning, including the vmPFC, hippocampus, and posterior cingulate cortex (PCC). The differential recruitment of reactive and cognitive fear circuitry was also associated with optimal escape decisions derived from a Bayesian model, emphasizing the SOS proposal of adaptive shifts between fear circuitry that helps to adjust behavior (1). These findings have provided compelling evidence for dissociation in the neural circuitry supporting threat responses, although the differential recruitment of cognitive and reactive fear circuits have yet to be incorporated in neurocognitive models for the learning and long-term memory of threat associations.

Accordingly, here we integrate theoretical perspectives from the predatory imminence model of predator–prey interactions (17) and the SOS hypothesis as supported by the video game literature (32) to propose that egocentric spatial distance of a conditioned threat will differentiate reactive and cognitive fear circuits during acquisition and extinction training that will impact behavioral indices of learning magnitude, extinction success, and susceptibility to fear reinstatement. Although the present investigation is focused on this distinction between "reactive" and "cognitive" fear circuitry to remain consistent with the terminology recently proposed by Mobbs et al. (32, 33), we acknowledge that these circuits do not serve single functions but reflect a complex interplay among mental processes that extend beyond threat learning and, despite having behavioral consequences, may not directly contribute to conscious feelings of fear (3). We nevertheless use the term "fear conditioning" to remain consistent with past literature in this area, recognizing that there is an active debate on the extent to which conditioning paradigms relate to the neural circuitry for fear experience (34–36). Central to this debate is whether fear can be traced to phylogenetically programmed neural circuits that are mirrored across species, or whether subjective fear is cognitively assembled by humans from higher-order representations orthogonal to lower-order defensive, physiological reactions (36). There is general consensus, however, that one means by which to improve our study of fear and potentially reconcile this debate is to further study the ecological conditions that dissociate different fear states, such as by studying the influence of threat imminence (33). Doing so can help develop a better understanding for underlying defensive survival circuits conserved across species, before determining how they contribute to the conscious feeling of fear. Therefore, detailing the distinction between cognitive and reactive states offers a means by which to provide more clarity to the general definition of fear, especially when translated to one of the most prominent means by which fear has been studied in the literature: fear conditioning.

In sum, the persistent effects of proximal threats on neural circuitry are implicated both theoretically and in the hypothesized mechanisms of PTSD, although they have yet to be examined in an empirical setting. This gap in the literature is particularly important to address, given critiques of the ecological validity of standard laboratory fear-conditioning paradigms as models of stress disorders (37, 38). We overcame the methodological limitation of manipulating threat proximity by adapting immersive 3D VR technology into the functional magnetic resonance imaging (fMRI) -scanning environment to simulate encountering a male avatar while walking down an alleyway. This technical advance allowed us to create ecologically valid (human conspecific) threats that either invaded peripersonal space—within arm's reach of the

participant (proximal/near threat)—or were presented at a farther distance (distal/far threat) in a first-person perspective. In addition, the virtual environment permitted multimodal manipulations of the acquisition and extinction contexts using unique auditory (ambient background noise) and visual (objects, color, texture, and lighting) background features. On day 1, one threat avatar at each distance was partially reinforced with aversive shocks (CS^+_{Near}, CS^+_{Far}), whereas another safe avatar was explicitly unreinforced (CS^-_{Near}, CS^-_{Far}). This procedure was followed by fear extinction (no reinforcement to any avatar) in a novel context (Fig. 1). The next day, participants returned for extinction recall in the virtual extinction context and fear reinstatement (unreinforced CS presentations following shock reminders) in the virtual-acquisition context. We isolated brain activation specific to the interaction of threat assessment and proximity by first comparing responses across threatening and safe avatars at near and far distances (e.g., $CS^+_{Near} > CS^-_{Near}$) and then comparing this fear-learning index across distances for each experimental phase. In doing so, our analyses focused on differences in threat response while controlling for low-level effects of distance, size, visual salience, and potential unconditioned threat responses (i.e., male in a dark alley).

Consistent with SOS and predatory imminence theories, we hypothesized that peripersonal threats would preferentially recruit reactive components of fear circuitry, whereas distal threats would preferentially recruit higher-order association (cognitive) areas, and that these differences would persist even when threat stimuli are no longer reinforced. Furthermore, because proximal threats evoke stronger defensive responses, we hypothesized that they would display an amplified conditioned fear response, greater resistance to extinction, and consequently, enhanced susceptibility to fear reinstatement. To test this latter hypothesis, we applied a multivariate fMRI approach that assessed the degree to which threat representations configured during acquisition persist throughout the extinction phase and, critically, whether this pattern similarity is predictive of a reinstated fear response the next day. This approach builds on previous work that has demonstrated increasing trial-by-trial similarity in neural representational patterns for reinforced stimuli during fear conditioning (39), and here we test whether the same patterns during acquisition are differentially maintained throughout extinction for near and far threats. By evaluating this change in acquisition-phase representational similarity throughout the extinction phase, we were able to better isolate neural regions with extinction-resistant representations, ultimately providing a more comprehensive understanding of proximal influences on fear memory.

Results

Threat Proximity Impacts Behavioral and Physiological Indices of Conditioned Learning.

Shock expectancy. Online ratings of shock expectancy revealed successful conditioning on day 1 (Fig. 2*A*) (CS-Type × Time interaction, $F_{1,\ 37} = 57.916$, $P < 0.001$, $\eta_p^2 = 0.61$), with higher ratings for CS^+ than CS^- avatars during late compared to early trials ($t_{37} = 7.610$, $P < 0.001$, Cohen's $d = 1.235$). This effect further interacted with distance (CS-Type × Distance × Time interaction, $F_{1,37} = 6.161$, $P = 0.018$, $\eta_p^2 = 0.143$), with a greater difference in conditioning for Near compared to Far conditions during early trials (CS-Type × Distance, $F_{1,37} = 11.874$, $P = 0.001$, $\eta_p^2 = 0.243$), but not late trials (CS-Type × Distance, $F_{1,37} = 0.377$ $P = 0.543$, $\eta_p^2 = 0.01$). Post hoc t tests confirmed that early acquisition was enhanced to near threats ($t_{37} = 3.446$, $P = 0.001$, Cohen's $d = 0.559$).

Analysis of extinction and extinction recall data showed intact safety learning and retention but no effect of distance (see *SI Appendix* for the full statistical report). During fear reinstatement, we found a significant CS-Type × Distance interaction (Fig. 3) ($F_{1,\ 37} = 7.701$, $P = 0.009$, $\eta_p^2 = 0.172$), such that the difference between CS^+ and CS^- ratings was higher for near than far threats ($t_{37} = 2.775$, $P = 0.009$, Cohen's $d = 0.45$). In sum, near threats demonstrated higher ratings of shock expectancy during early acquisition on day 1 and during reinstatement on day 2. Analysis of response times for the ratings showed participants were equally fast at making ratings for near and far avatars, suggesting that far avatars were not more difficult to discern (see *SI Appendix* for more details).

Skin conductance response. Skin conductance response (SCR) analyses also revealed successful conditioning on day 1 (Fig. 2*B*) (main effect of CS-Type, $F_{1,30} = 27.976$, $P < 0.001$, $\eta_p^2 = 0.483$; CS-Type × Time interaction, $F_{1,\ 30} = 4.384$, $P = 0.045$, $\eta_p^2 = 0.127$), with higher SCRs to CS^+ than CS^- avatars during early compared to late trials ($t_{30} = 2.094$, $P = 0.045$, Cohen's $d = 0.376$). Distance interacted with CS-Type ($F_{1,\ 30} = 4.422$, $P = 0.044$, $\eta_p^2 = 0.128$), such that SCRs were differentially greater ($CS^+ > CS^-$) for near threats than far threats ($t_{30} = 2.103$, $P = 0.044$, Cohen's $d = 0.378$). Although the three-way interaction was not significant (CS-Type × Distance × Time, $F_{1,\ 30} = 2.667$, $P = 0.113$, $\eta_p^2 = 0.082$), the difference between near and far threats was significant during early trials ($t_{30} = 2.173$, $P = 0.038$, Cohen's $d = 0.39$) but not late trials ($t_{30} = 0.558$, $P = 0.581$, Cohen's $d = 0.1$).

Near threats were also more resistant to extinction learning (CS-Type × Distance × Time, $F_{1,\ 30} = 4.777$, $P = 0.037$, $\eta_p^2 = 0.137$). The difference between near and far threats was greater during early than late extinction trials ($t_{30} = 2.186$, $P = 0.037$, Cohen's $d = 0.393$), such that differential SCRs ($CS^+ > CS^-$) between near and far avatars decreased from early ($t_{30} = 2.031$, $P = 0.051$, Cohen's $d = 0.365$) to late ($t_{30} = 0.282$, $P = 0.780$, Cohen's $d = 0.051$) trials. Otherwise, SCRs indicated successful extinction learning and retention, with no significant main effect of CS-Type during extinction learning on day 1 ($F_{1,\ 30} = 0.946$, $P = 0.339$, $\eta_p^2 = 0.031$; CS-Type × Time interaction, $F_{1,\ 30} = 0.162$, $P = 0.691$, $\eta_p^2 = 0.005$) or during extinction recall on day 2 ($F_{1,\ 30} = 1.581$, $P = 0.218$, $\eta_p^2 = 0.05$). Unlike the shock-expectancy data, we found no evidence for significant reinstatement of SCRs on day 2 (CS-Type main effect, $F_{1,\ 30} = 0.057$, $P = 0.812$, $\eta_p^2 = 0.002$; all other CS-Type interactions, $P > 0.05$). In sum, analysis of skin conductance data revealed that near threats elicited greater SCRs than far threats during early acquisition and showed an initial resistance to extinction learning.

Near and Far Threats Engage Distinct Neural Circuitry.

We next evaluated whether differences in the spatial proximity of conditioned threats align with Mobbs et al.'s distinction between reactive and cognitive fear circuits in the brain (32, 33). For the univariate analysis of fMRI data during fear acquisition, we first investigated CS^+/CS^- differences within Near and Far conditions separately, split into early and late trials. While no clear differences emerged for early trials, we did find robust increased activation in late trials for both near and far CS^+ stimuli when compared to their respective CS^- stimuli (Fig. 4*A* and *SI Appendix*, Table S1). This increased activation was observed for both conditions in the bilateral insula and frontopolar PFC (BA10). For near threats ($CS^+_{Near} > CS^-_{Near}$), we also observed increased activation in the right cerebellum, anterior midcingulate cortex (aMCC), and thalamus, with clusters encompassing anterior midbrain regions, such as the ventral tegmental area and substantia nigra. Moreover, the increased activation in the aMCC, thalamus, and midbrain observed for near threats was significantly greater when compared to far threats (for an axial view of the midbrain, see also Fig. 6*A*). Functional connectivity analyses further revealed differences related to threat proximity primarily during late trials (Fig. 4*B*). In particular, far threats demonstrated greater coupling of the amygdala, hippocampus, and vmPFC with precuneus, presupplementary motor area (pre-SMA), and premotor regions when compared to near threats. Thus, when evaluated together, the activation and connectivity

differences during acquisition suggest distinct neural profiles for near and far threats that closely resemble the recently proposed distinction between reactive (aMCC and midbrain) and cognitive (amygdala, hippocampus, and vmPFC) fear circuits.

During extinction, near and far threats continued to display differential effects of CS-Type (Fig. 5*A* and *SI Appendix*, Table S2). In early trials, near threats ($CS^{+}_{Near} > CS^{-}_{Near}$) recruited the left primary motor cortex (postcentral gyrus) and presented with greater activation, when compared to far threats ($CS^{+}_{Far} > CS^{-}_{Far}$), in the left posterior operculum. In comparison, the main effect of far threats in early trials only exhibited activation in the PCC. During late trials, activation associated with near threats shifted to the cerebellum, whereas far threats recruited large clusters of activation encompassing the dorsomedial PFC, subgenual ACC, orbitofrontal cortex (OFC), and left anterior insula. Activation in the left anterior insula was also greater for far threats when compared to near threats.

Analysis of whole-brain functional connectivity revealed differences between near and far threats in early- and late-extinction trials. In early extinction, near threats displayed greater amygdala–right motor cortex, PAG–precuneus, and vmPFC–frontopolar cortex connectivity when compared to far threats. Alternatively, far threats displayed greater amygdala connectivity with the anterior medial PFC, right lateral occipital cortex, and right middle temporal gyrus in late-extinction trials (Fig. 5*B*). The activation and connectivity effects during extinction therefore show a differential neural response to near and far threats that extended beyond just the initial learning of threat associations during acquisition.

Multivariate Cerebellar Representations during Extinction Predict Behavioral Reinstatement Response to Near Threats. The behavioral findings suggested that near threats are more susceptible to fear reinstatement than far threats, despite similar rates of extinction learning. This effect may result from persistent neural representations of the threat value of proximal CSs in reactive fear circuits that are difficult to detect with standard univariate approaches. Whole-brain functional activation results from acquisition and extinction only revealed consistent recruitment of right cerebellar lobule VI for the $CS^{+}_{Near} > CS^{-}_{Near}$ contrast (Fig. 6*A*). To assess whether this finding was representative of a persistent threat response, we conducted a post hoc multivariate analysis in right cerebellar lobule VI using a representational similarity analysis (RSA) approach (see *Materials and Methods* for details). This analysis sought to show how conditioned fear representations of each CS^{+} at the end of acquisition training changed through extinction (Fig. 6*B*), thereby providing a means by which to relate the maintenance of threat representations at day 1 to the enhanced behavioral reinstatement for near threats a day later. Thus, while our initial univariate approach confirmed general neural differences between near and far threats, here we sought to explicitly test whether extinction–acquisition pattern similarity in cerebellar representations further delineate the longer-term consequences of spatial proximity on fear memories.

A significant Time × Distance interaction was found ($F_{1, 39} = 12.333$, $P = 0.001$, $\eta_p^2 = 0.24$), such that only CS^{+}_{Far} exhibited an increase in pattern dissimilarity from the beginning to the end of extinction ($t_{39} = 4.967$, $P < 0.001$, Cohen's $d = 0.785$). This result implicates a change in the threat representation accompanying extinction learning. In contrast, CS^{+}_{Near} did not show a significant change in dissimilarity ($t_{39} = 0.850$, $P = 0.401$, Cohen's $d = 0.134$), suggesting a persistence of the threat representation that was resistant to extinction learning. To assess whether extinction learning-related representational dissimilarity had consequences for fear reinstatement the next day, we regressed the same RSA dissimilarity metric from the end of extinction training with differential shock-expectancy ratings from early reinstatement. For both Near and Far conditions, less dissimilarity (a more similar threat representation of the CS^{+} from the end of acquisition to the end of extinction) was associated with greater fear reinstatement (Fig. 6*B*) (Near: $r = -0.390$, $P = 0.016$; Far: $r = -0.356$, $P = 0.028$). Thus, not only were persisting multivariate cerebellar representations throughout extinction learning more likely for near threats, the similarity of these representations from the end of acquisition training to the end of extinction training also predicted the likelihood of fear reinstatement a day later. Subsequent analyses showed that these effects were selective to the cerebellum (*SI Appendix*, Table S3).

A similar Time × Distance interaction effect was observed for the CS^{-} events ($F_{1, 39} = 5.222$, $P = 0.028$, $\eta_p^2 = 0.118$) (*SI Appendix*, Fig. S2), such that the CS^{-} representation encoded at the end of acquisition changed throughout extinction in the Far condition ($t_{39} = 3.653$, $P < 0.001$, Cohen's $d = 0.578$), but not in the Near condition ($t_{39} = 0.286$, $P = 0.776$ Cohen's $d = 0.045$). CS^{-} representational dissimilarity at the end of extinction was only significantly associated with fear reinstatement in the Near

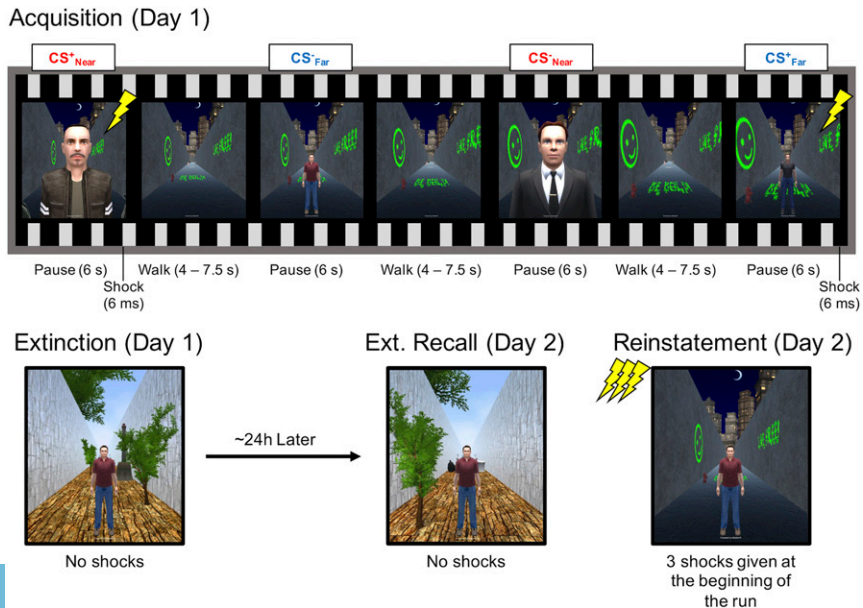

Fig. 1. Experimental design. An example of the trial sequence is shown for the acquisition phase. Participants were placed in a 3D VR context consisting of a long alleyway corridor and passively guided in a forward direction until a human avatar appeared. During fear acquisition, two avatars at each distance coterminated with a brief electrical shock (CS^{+}_{Near} and CS^{+}_{Far}), while two avatars were explicitly unreinforced (CS^{-}_{Near} and CS^{-}_{Far}). After the acquisition phase, participants were exposed to the same stimuli in a new context, without shock reinforcement, in order to promote fear-extinction learning. A day later, participants returned for extinction recall in the same extinction context, and fear reinstatement in the original acquisition context. Fear reinstatement began with three shocks prior to the presentation of human avatars. Each phase consisted of 40 character presentations, 10 per condition.

condition ($r = -0.432$, $P = 0.007$) and not in the Far condition ($r = 0.129$, $P = 0.439$). Collectively, these multivariate analyses emphasize a cerebellar component to the reactive fear circuit that is important for differentiating threat and safety representations across learning contexts and may contribute to the vulnerability of proximal threat memories to fear reinstatement.

Discussion

The present study demonstrates that conditioned threats engage different fear-learning and extinction mechanisms in the human brain depending on spatial proximity in egocentric space. Using an innovative immersive 3D VR paradigm adapted for the fMRI scanning environment, we showed that when conspecific threats breach peripersonal space, they engage a reactive fear-learning circuit that makes proximal threat associations more resistant to extinction processes and more susceptible to subsequent fear renewal. Our findings have important implications for rethinking how the classic neurobiological model of fear conditioning informs clinical observations of fear persistence. In particular, we report a contribution of brain areas that organize defensive reactions in near-body space and learn from these encounters, which is especially relevant for PTSD, given that invasion of bodily space is a key hallmark of index traumas that lead to this disorder (14–16).

Collectively, our behavioral and neural results indicate enhanced fear acquisition to proximal threats, with corresponding increases in activation in the motor region of the CC (aMCC) and portions of the thalamus and midbrain. Moreover, the change in differential SCR ($CS^+ > CS^-$) from early to late extinction was larger for near threats than far threats, indicating a delay in engaging successful extinction processes when threats invaded peripersonal space. While this effect was small, its significance is noteworthy when coupled with evidence of neural differences during extinction and subsequent effects at reinstatement. During extinction, distal threats engaged cortical fear circuitry more than proximal threats, whereas proximal threats continued to elicit cerebellar activity whose multivariate representation of the acquired threat value of the CSs persisted throughout extinction learning. This cerebellar signature of extinction-resistant threat predicted the magnitude of behavioral fear reinstatement the next day, and proximal threats were more susceptible to fear reinstatement than distal threats.

Our findings during fear acquisition align with the distinction between cognitive and reactive fear circuits derived from nonhuman animal predation studies and human studies of chase-and-capture video games (25–28, 32), which served as the primary framing hypothesis of the present study. We show here that this neurobiological distinction emerges as humans acquire and extinguish threat associations during fear-conditioning tasks. Proximal threats were preferentially associated with aMCC, midbrain, and thalamic activity, implicating recruitment of survival circuitry that coordinates defensive action (26). Moreover, while proximal threats did not specifically elicit greater activation in the PAG—perhaps due to the inability of participants to fully engage flight mechanisms given the nature of the task and constraints within the scanning environment—they did recruit greater midbrain activity encompassing the ventral tegmental area and substantia nigra, dopaminergic brainstem nuclei that display reciprocal connections with the PAG (40–43), gate information sent to the PFC (44), and shape adaptive fear-learning behavior (45). In contrast, functional connectivity analyses revealed that distal threats displayed greater connectivity of the amygdala, hippocampus, and vmPFC with higher-level cortical regions, such as the pre-SMA and precuneus, often related to complex action planning/preparation and visuo-spatial information

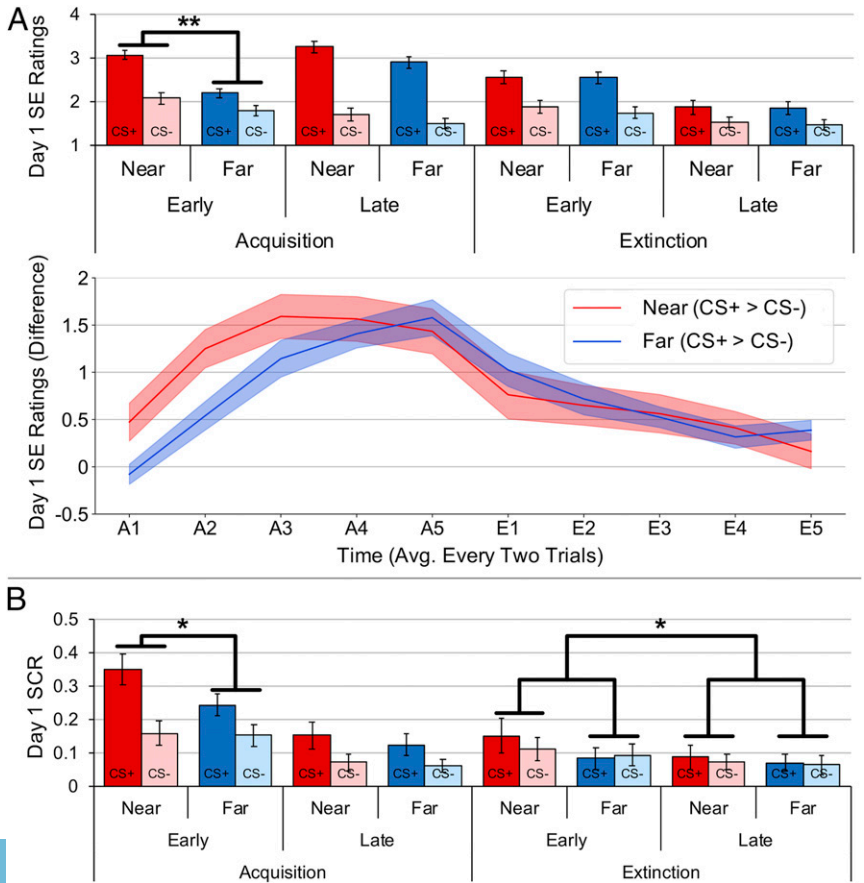

Fig. 2. Shock expectancy (SE) ratings and SCR during fear acquisition and extinction on day 1. Compared to far threats, near threats showed greater SE ratings (*A*) and SCR (*B*) during early fear-acquisition trials, as well as a delayed reduction in SCR during extinction. Bars and shaded areas represent SEM. $*P < 0.05$, $**P < 0.01$.

processing (46–48). Collectively, the findings from fear acquisition support the notion that near threats invading peripersonal space are more likely to elicit neural activity associated with a circa-strike reaction to imminent threat, whereas distributed cortical connections observed for far threats enable recruitment of neural mechanisms underlying cognitive avoidance or coping strategies (1).

Near threats did not continue to elicit greater aMCC, thalamic, or midbrain activity during extinction when shocks were no longer reinforced, suggesting that recruitment of the full reactive fear circuit may be specifically related to the initial learning and explicit reinforcement of a threat stimulus. Activation effects for near threats during extinction were observed in the primary motor cortex and cerebellum, whereas far threats continued to recruit cognitive fear circuitry and canonical regions often engaged during extinction learning, including the PCC, OFC, insula, and dorsomedial PFC, which parallels some of the effects observed during fear acquisition to both near and far threats. Even though this overlap in network engagement during acquisition and extinction is consistently observed in the literature (49), the reengagement of these regions in our univariate analyses does not necessarily suggest they are performing the same functions or that their activation is specifically threat related. That is, whereas greater activation in these regions during acquisition supports the configuration of a threat-associative memory, during extinction a new safety association is hypothesized to form that competes with the existing memory to help diminish fear responses (50), which likely draws upon a similar network of regions to facilitate this associative learning.

The added recruitment of the PCC and OFC during extinction for far threats further supports this interpretation, given that these regions are consistently more active for the CS^-, compared to the CS^+, during acquisition when the CS^- is initially learned to be safe (51). Moreover, OFC activation has been specifically proposed to signal safety by tracking the increasing distance to a threat stimulus (52), suggesting that this region might especially be relevant for fear extinction to far threats. The notion that far threats are more susceptible to reinterpretation as a safe stimulus during extinction learning is further evidenced by greater amygdala–mPFC connections during late extinction, as well as greater recruitment of dorsolateral prefrontal regions during extinction recall (*SI Appendix*, Fig. S1), both of which are frequently found in other fear-extinction and regulation studies (49). According to the SOS model, this effect is likely driven by more successful engagement of prediction and threat assessment systems when threats are distal, allowing for goal-directed actions to optimize escape and initiate feelings of safety (1). Thus, despite a lack of behavioral differences between near and far threats during extinction, far threats nonetheless demonstrate activation and connectivity effects that suggest improved recruitment of extinction mechanisms, which may have contributed to their faster SCR extinction profile and to a more subdued reinstatement response the next day.

Our results also provide evidence for a key role of the cerebellum in the extinction of proximal threats and in predicting fear reinstatement. While the univariate analysis revealed consistently greater activation within right cerebellum lobule VI during the acquisition and extinction phases—which also resurfaced during fear reinstatement (*SI Appendix*, Fig. S1)—the multivariate RSA emphasized that this region is particularly relevant for the maintenance of proximal threat representations. Both CS^+_{Near} and CS^-_{Near} cerebellar representations were more resistant to change throughout extinction than CS^+_{Far} or CS^-_{Far} representations, and this lack of change associated with fear renewal susceptibility a full day later, suggesting a role for the cerebellum in maintaining the dissociation between safe and threat proximal stimuli across learning contexts. These findings were revealed by relating a multivariate assessment of representational similarity across acquisition and extinction with behavioral fear reinstatement, an approach that provides a more detailed evaluation of extinction learning success. We tested this association within the cerebellum, given that our univariate analyses revealed recapitulated activation in this region for near threats during extinction. The RSA effect was found only in the cerebellum and not in our other regions-of-interest (ROI) (*SI Appendix*, Table S3). Taken together, our univariate and multivariate analyses indicate that the distinction between cognitive and reactive fear circuitry configured by threat proximity is evident during the intial acquisition of threat associations, while suggesting that the cerebellum should be included in an expanded model of reactive fear, which is particularly relevant for the maintenance of proximal threat associations.

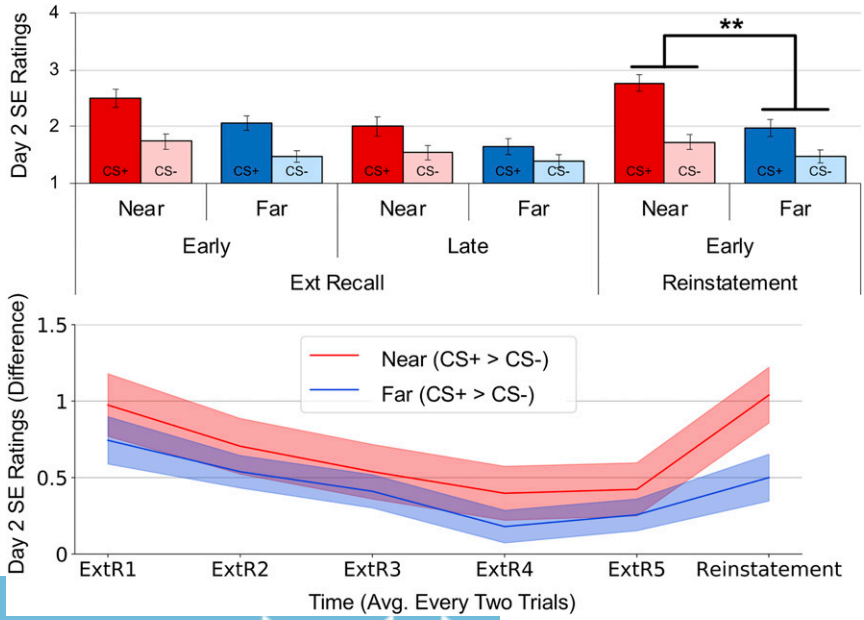

Fig. 3. SE ratings from day 2 revealed that near threats were more likely to reinstate a fear response. Although near and far threats displayed similar ratings throughout extinction recall, a significant difference emerged during early reinstatement trials. Bars and shaded areas represent SEM. $^{**}P < 0.01$.

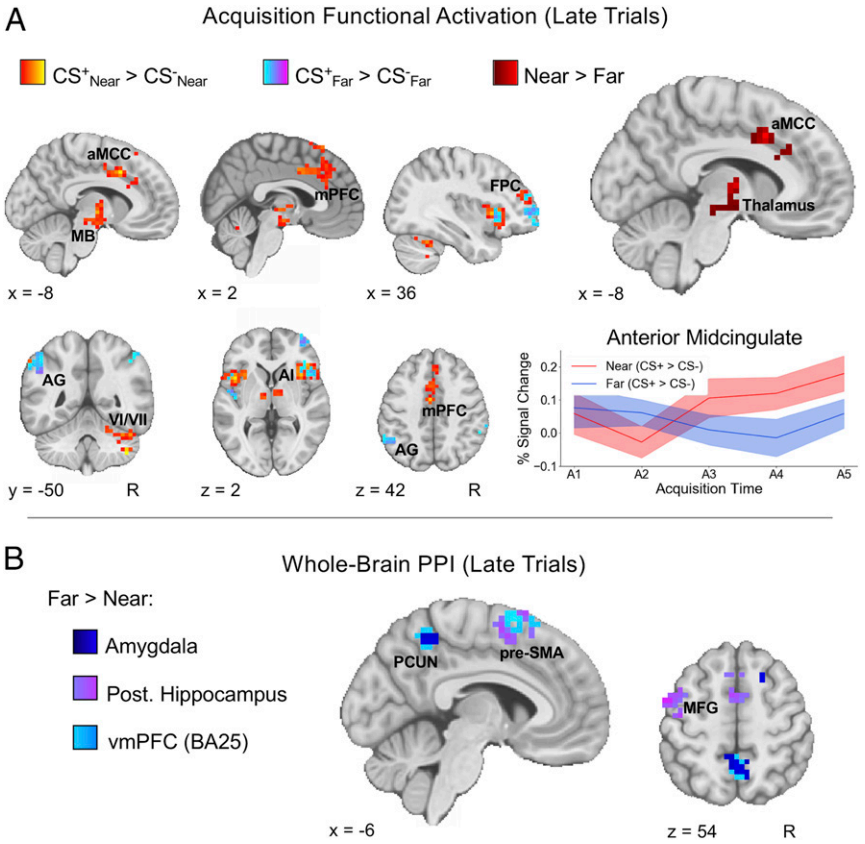

Fig. 4. Near and far threats elicit distinct functional activation and connectivity during fear acquisition. (*A*) During late acquisition, near and far threats displayed increased activation in bilateral anterior insula (AI) and frontopolar cortex (FPC), with far threats eliciting unique activation in lateral parietal regions such as the angular gyrus (AG) and near threats eliciting unique activation in mPFC, midbrain (MB), and cerebellar lobules VI and VII. The direct comparison between near and far [(CS^{+}_{Near} > CS^{-}_{Near}) > (CS^{+}_{Far} > CS^{-}_{Far})] revealed increased activation for near threats in the aMCC and thalamus, extending into anterior MB regions. Greater aMCC activity for near threats occurred relatively early during acquisition, shown by a steep increase in percent signal change from the second to third pair of trials (extracted from a 6-mm spherical ROI centered on the maximum *z*-statistic voxel for the aMCC Near > Far cluster). Shaded areas represent SEM. (*B*) PPI analyses revealed similar connectivity patterns for amygdala, hippocampus, and vmPFC seeds. Far threats (CS^{+}_{Far} > CS^{-}_{Far}) consistently displayed increased coupling of these ROIs with medial and lateral cortical regions, including the pre-SMA, precuneus (PCUN), and middle frontal gyrus (MFG) when compared to near threats (CS^{+}_{Near} > CS^{-}_{Near}). All statistical maps represent group results after mixed effects analysis (z > 2.3, cluster-corrected P < 0.05).

Although the cerebellum has been underemphasized in traditional fear-conditioning models, cerebellar activity is related to the potentiated startle effect (53–55) and growing evidence implicates the cerebellum in learning and extinction of fear memories (49, 56–60). Only combined amygdala and cerebellar vermis blockade promotes amnesia for strong fear memories (61), suggesting that the cerebellum is an important region to consider in the maintenance of fear representations. Another line of research has also implicated PAG–cerebellar links (via the inferior olivary nucleus) as an additional component in the neural circuitry that configures defensive response to aid survival in threatening situations (21), whereby the PAG effectively

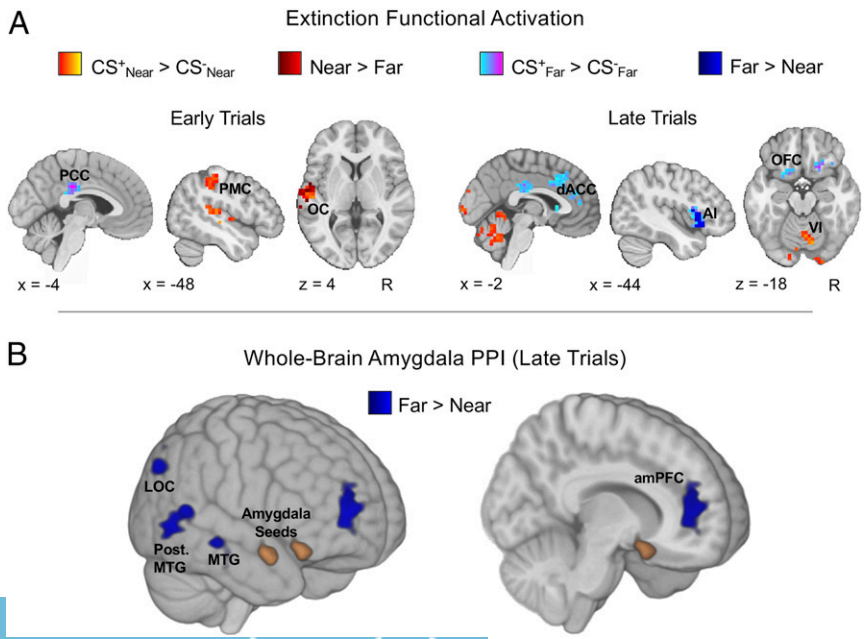

Fig. 5. Near and far threats continue to display differences in functional activation and connectivity during fear extinction. (*A*) Differences in neural activation between near and far threats were observed during early and late trials of extinction. The independent CS^{+} > CS^{-} contrasts for both Near and Far conditions revealed that near threats were more likely to recruit activation in the primary motor cortex (PMC), opercular cortex (OC), and cerebellum (lobule VI), whereas far threats were more likely to recruit activation in the PCC, dorsal ACC, OFC, and anterior insula (AI). (*B*) PPI analysis of late extinction trials showed greater amygdala connectivity with the amPFC, right lateral occipital cortex (LOC), and right middle temporal gyrus (MTG) for far threats. Three-dimensional images are displayed without volume occlusion. All statistical maps represent group results after mixed-effects analysis (z > 2.3, cluster-corrected P < 0.05).

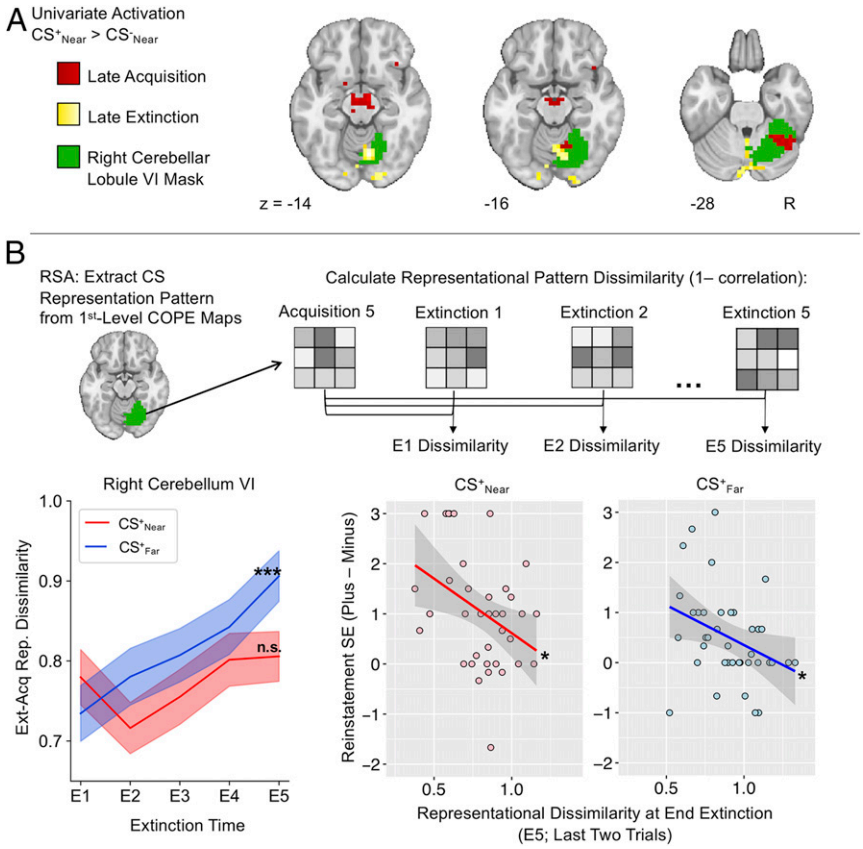

Fig. 6. Near threats promote persistent threat representations in the cerebellum during extinction. (*A*) Univariate results of acquisition and extinction for the $CS^{+}_{Near} > CS^{-}_{Near}$ contrast displayed consistent activity within right cerebellar lobule VI. (*B*) Activity patterns specific to the threat stimuli were extracted from the CS^{+}_{Near} and CS^{+}_{Far} contrast of parameter estimate (COPE) images during late acquisition within the right cerebellar lobule VI. CS^{+} representations during extinction were compared to these acquisition threat representations, revealing increased dissimilarity from the beginning (E1) to the end (E5) of extinction only for the Far condition. Shaded areas represent SEM. Dissimilarity metrics of extinction learning (from the end of extinction compared to the end of acquisition) negatively correlated with shock expectancy ratings during early fear reinstatement trials the next day. $*P < 0.05$; $***P < 0.001$; n.s., not significant.

controls and coordinates motor output through connections to the cerebellum (20). Accordingly, investigations of cerebellar topography with fMRI have revealed evidence for affective and sensorimotor representations in lobules V/VI (62–65), further emphasizing a need to better incorporate the contribution of the cerebellum to models of threat behavior in humans.

Our results show that reactive fear circuit engagement is particularly evoked in the initial learning and reaction to a near threat, while activity patterns in the cerebellum maintain those threat representations despite evidence of behavioral extinction learning, suggesting that the cerebellum should be incorporated into existing models of reactive fear circuitry. This maintained threat representation, combined with less recruitment of cognitive avoidance and extinction-learning circuity, induces susceptibility to a reinstated fear response when reencountering near threats in a dangerous context. The present study thus provides a finding that dissociation in cognitive and reactive fear circuitry can inform the way in which threat associations are learned and remembered, adding to mounting evidence for dissociable fear states based on ecological context (33). These findings may also have important translational impact in redirecting clinical focus from the more traditional fear-extinction circuitry in the vmPFC, amygdala, and hippocampus to the cerebellum as a possible site of therapeutic intervention to prevent fear recovery in anxiety and stress disorders triggered by near-body traumas. Finally, our results highlight the methodological advance of using 3D immersive VR in the scanning environment to evaluate the influence of threat imminence. Our approach presented stimuli in a first-person, egocentric perspective that allowed near threats to invade peripersonal space as they appeared to project outward from the screen. In contrast to 2D studies of proximity effects on neural circuit engagement during video games, this immersive VR experience instils a feeling of "presence" for the participants and, consequently, the real-world relevance of our findings (66). Future studies that also capitalize on this approach may be better equipped to evaluate the configuration of interpersonal defensive boundaries (31, 67).

Limitations. While the present study provides an evaluation of associative learning for proximal and distal threats, a number of methodological and conceptual limitations will need to be addressed in future work. The present experiment was designed to specifically test how spatial proximity configures differences in the initial appraisal and subsequent memory for threats, although the influence of proximity on fear conditioning may be characterized in other ways, such as temporal proximity (32). Although we paired conditioned stimuli to aversive shock, social stimuli that invade peripersonal space naturally evoke enhanced defensive responses (31), and recent evidence suggests that innate and learned threats have different behavioral consequences that might be supported by dissociable neural pathways (30). Accordingly, future studies that evaluate the influence of proximity on fear memories by considering alternative stimuli or means of associative learning, such as social mechanisms via observation (68), might aid the interpretation of the effects reported here.

Furthermore, while the neural differences we identified may have contributed to the observed behavioral and physiological effects, future studies should strive to assay diverse motor output metrics directly to support this interpretation, taking into consideration the movement constraints of the fMRI scanning environment. Similarly, although this pattern of results corroborates the effects predicted by predatory imminence theory, near threats in our experimental design might have been perceived as more compatible with aversive shock than far threats, contributing to more rapid acquisition of near threats during early acquisition. Nevertheless, both near and far threats were learned successfully by late

acquisition, eliciting similar ratings of shock expectancy even after accounting for responses to the nonreinforced stimuli. The use of a consistent shock reinforcer therefore allowed us to examine the extinction and reinstatement response of proximal and distal threats without the confound of differential learning success. The ecological validity of this approach is supported by evidence that proximity of trauma is associated with the subsequent distress of PTSD symptoms (14–16, 69). While predatory imminence theories suggest the threat value of the cues primarily drive the behavioral and neural effects observed here, we acknowledge that contextual or attentional factors may also contribute to this dissociation in neural circuitry. Future work is needed to pinpoint the exact mechanisms contributing to this neural circuit shift.

While both shock expectancy and skin conductance demonstrated similar effects during early acquisition, they diverged in subsequent extinction and reinstatement phases. Our findings suggest that during extinction, participants experienced a more sustained arousal response to previously acquired threats in near-body space, even if they did not necessarily rate these proximal CS as more likely to elicit a threat. During reinstatement, we found the opposite effect, whereby participants appraised the threat value of proximally CS to be higher than that of their distal counterparts, even though SCR was comparable between the two. This similarity and divergence in our data emphasize the multifaceted nature of fear and that subjective expectancy ratings do not directly map onto psychophysiological response (70). In fact, a recent multivoxel pattern analysis suggests this dissociation in self-reported fear and physiological reactivity is reflected in distinct neural representations, whereby the dorsomedial and lateral PFC are more involved in predicting subjective fear response, while the amygdala and insula are more involved in predicting physiological reactivity (71). In designing the present study, we collected expectancy ratings to measure contingency learning and explicit knowledge of threat associations, while SCR was used to index an arousal response that may or may not align with cognitive expectations. Thus, we acknowledge that neither of these measures were able to fully capture participants' phenomenological experiences. Rather, they should be interpreted collectively with the neural findings to aid in understanding differences in proximal and distal threat appraisal. However, future studies may benefit from directly measuring subjective fear reports to more precisely determine how dissociation between cognitive and reactive neural recruitment might contribute to fear experience.

Ultimately, these limitations highlight the conceptual debate concerning whether phylogenetically conserved neural circuits support the conscious feeling of fear (36). In recent years, this issue has motivated a shift toward utilizing more ecologically valid paradigms that can delineate different forms of fear, in the hope that such an approach might clarify the contexts that support these fear states, as well as the relationship between the engagement of defensive survival circuits and actual fear experience (32, 33). The present study provides an important contribution to this endeavor by validating the neuropsychological distinction between cognitive and reactive fear circuits, while also translating the influence of threat imminence into the fear-conditioning domain in humans.

Conclusions

In conclusion, these findings provide a detailed assessment of underlying neural circuitry modulated by threat proximity across fear learning, extinction, and reinstatement. They also illustrate the added value of immersive VR applications in the fMRI scanning environment. Our results extend prior animal predation and human video game work on threat imminence to the fear-learning domain and highlight the amplified acquisition and impaired extinction of threats invading peripersonal space. Given the influence of proximity on PTSD diagnosis and symptom severity (14–16, 69), the current findings suggest differential treatment options based on initial proximity to a traumatic event and implicate cerebellar maintenance of proximal threat representations as a potential target for therapeutic interventions.

Materials and Methods

Participants. Forty-nine participants were recruited from the Duke Brain Imaging and Analysis Center subject pool. All participants completed written informed consent prior to participation in the study, and received monetary compensation for their time ($20/h). The study was approved by the Duke University Health System Institutional Review Board. Participants were right-handed and had normal or corrected-to-normal vision. Five participants withdrew early from the study and did not return for day 2. Four participants were excluded due to technical issues during scanning related to the 3D environment (i.e., television and glasses) or the administration of aversive shocks. Thus, the final sample used in the neuroimaging analyses consisted of 40 participants ($mean_{age} \pm SD = 24.55 \pm 4.16$; 18 female).

Materials.

VR contexts and stimuli. Four 3D environments, all consisting of a long, narrow alleyway corridor, were used as contexts for the fear-conditioning phases. These environments were created in Unity (Unity Technologies) and consisted of two walls, a floor, and a sky presented in a first-person perspective. Four unique contexts were created with different wall and floor textures, lighting, skylines, and ambient background noise (e.g., street traffic). These contexts also contained pseudorandomized placement of unique contextual cues located along the alleyway corridor, such as trash cans, benches, and light posts. While in the virtual environment, participants were passively guided at 0.3 m/s along a forward path down the alleyway, which paused for 6 s during the presentation of stimuli.

CS and unconditioned stimuli (US) consisted of four distinct male human avatars exhibiting neutral facial expressions. The avatars suddenly appeared in the full-frontal view of the research participant as they navigated down the alleyway, remained static during presentation, and disappeared from view after 6 s. Participants' travel within the virtual environment was paused for the duration of the CS avatar presentations. For the near trials, the avatars appeared at an interpersonal distance of 0.6 m, while for the far trials they appeared at 3 m. The VR simulation maintained proper spatial distance cues such that avatars were appropriately sized according to their distance from the participant.

The virtual contexts and stimuli were displayed on a Magnet Vision 3D television (Resonance Technology) and shown to the participants via an angled, first-surface mirror attached to the MR head coil. To create the 3D effect, participants wore MRI-compatible 3D glasses, which created the illusion that near stimuli projected outward from the screen into peripersonal space, whereas far stimuli appeared at a distance.

Procedure. The study was split into two sessions that took place on separate days (~24 h between the two sessions). On day 1, following informed consent, US shock intensity was calibrated for each participant to be annoying but not painful using an ascending staircase procedure developed in our laboratory (9). Participants then completed CS habituation, fear-acquisition, and fear-extinction phases during fMRI. Each of these phases occurred in a separate virtual context and presented four human avatars, two near and two far, split into CS^+ and CS^- conditions. Presentation order was structured such that no avatars appeared more than twice in a row. The avatars were pseudorandomly assigned to the CS-Type conditions across participants to avoid potential confounds of particular avatars with CS-Type assignment. Participants were told they would be passively guided along the virtual environment and that some avatars were dangerous (result in a brief shock), but participants were not told which avatars were dangerous or safe. In each phase, participants were passively guided along one of the alleyway contexts during the variable interstimulus intervals (4 to 7.5 s), and paused for the 6 s that an avatar appeared on screen. During the habituation phase, each avatar was presented twice to familiarize participants with the experimental set-up (data from this phase are not reported). During all other phases (acquisition, extinction, extinction recall, fear reinstatement), each avatar was presented 10 times, for a total of 40 avatar presentations. Five CS^+_{Near} and five CS^+_{Far} presentations coterminated with the US (50% partial reinforcement) during fear acquisition. Following fear acquisition, participants completed fear extinction with no shocks in a novel context. On day 2, shock intensity was set to the same level that was used during day 1. The participants completed extinction recall in the extinction context followed by fear reinstatement in the acquisition context. Reinstatement began with

three uncued shocks separated by 2 s each, prior to any presentation of CS avatars. The contexts used for the different phases were counterbalanced across participants.

US Delivery. Shock administration was controlled with the MP-150 BIOPAC system (BIOPAC Systems) using the STM200 Constant Voltage Stimulator. Electrical stimulation was applied transcutaneously over the median nerve of the right wrist and lasted for 6 ms, via a pair of general-purpose, MRI-compatible electrodes filled with conductive saline gel (Parker Laboratories).

US Expectancy Ratings. For each character presentation, participants rated via an MRI-compatible button box the perceived shock likelihood (shock expectancy) on a scale from 1 to 4: 1 being "definitely unlikely," 2 "somewhat unlikely," 3 "somewhat likely," and 4 "definitely likely." These ratings were recorded for each phase and served as a subjective behavioral measure of fear learning. Due to technical issues, two subjects during acquisition, one subject during extinction recall, and two subjects during reinstatement failed to record shock-expectancy ratings and were therefore excluded for shock-expectancy analyses of these phases.

SCRs. Skin conductance recording was controlled with the MP-150 BIOPAC system (BIOPAC Systems) via Ag/AgCl disposable electrodes placed on the palmar surface of the left hand. SCR analysis was performed with the Autonomate program (72) in MATLAB (The Mathworks) and scored responses if the trough-to-peak response occurred 1 to 4 s following stimulus onset, lasted between 0.5 and 5.0 s, and was greater than 0.02 microSiemens, following analyses previously described (73). Trials that did not meet these scoring criteria were scored as a zero. Prior to statistical analyses, the SCRs to CS were first normalized to the average US response within each subject. In order to ensure that our SCR analysis was appropriate for investigating differences in physiological arousal between CS^+ and CS^- (modulated by proximity), we excluded nine nonresponders who did not display any measurable levels of skin conductance to the US during acquisition, resulting in a final sample size of $n = 31$ for these analyses.

MRI Data Acquisition. Neuroimaging data were acquired on a 3T General Electric MR740 scanner with an eight-channel head coil at the Duke University Brain Imaging and Analysis Center. High-resolution T1-weighted structural scans were acquired using a 3D fast SPGR pulse sequence (repetition time [TR] = 8.16 ms; echo time [TE] = 3.18 ms; image matrix = 256^2; voxel size = 1 × 1 × 1 mm). Whole-brain functional scans were acquired for each experimental phase (acquisition, extinction, extinction recall, and reinstatement) parallel to the AC-PC line using a SENSE spiral-in sequence (TR = 2 s; TE = 27 ms; image matrix = 64^2; field-of-view = 256^2; slice thickness 3.8 mm; voxel size = 4 × 4 × 3.8 mm, 34 slices with interleaved acquisition, flip angle = 60°). To ensure MR signal stabilization, the first four TRs of each functional scan were excluded from analyses.

Neuroimaging Analyses.

Preprocessing. All neuroimaging data were preprocessed with FMRIPREP v1.0.15 (74, 75), a Nipype (76, 77) -based tool. T1-weighted anatomical images were corrected for intensity nonuniformity using N4BiasFieldCorrection v2.1.0 (78) and skull-stripped using antsBrainExtraction.sh v2.1.0 (using the OASIS template). The images were spatially normalized to the ICBM 152 Nonlinear Asymmetrical template v2009c (79) using nonlinear registration with the antsRegistration tool of ANTs v2.1.0 (80) with brain-extracted versions of both T1w volume and template. Cerebrospinal fluid, white-matter, and gray-matter segmentation were performed on the brain-extracted T1w using FAST (81) from FSL v5.0.9.

Preprocessing of functional data included slice timing correction with 3dTshift from AFNI v16.2.07 (82) and motion correction with MCFLIRT (83) in FSL. This step was followed by coregistration to the corresponding T1w using boundary-based registration (84) with 9 degrees-of-freedom, using FSL's FLIRT. The motion-correcting transformations, blood-oxygen-level-dependent (BOLD)-to-T1w transformation and T1w-to-template warp were concatenated and applied in a single step with antsApplyTransforms (ANTs v2.1.0) using Lanczos interpolation.

Frame-wise displacement (85) was calculated for each functional run using the implementation of Nipype. ICA-based automatic removal of motion artifacts (AROMA) was used to generate aggressive noise regressors as well as to create a variant of data that is nonaggressively denoised (86). Many internal operations of FMRIPREP use Nilearn (87), principally within the BOLD-processing workflow. For more details of the pipeline, see http://fmriprep.readthedocs.io/en/latest/workflows.html. Following FMRIPREP, the preprocessed output was skull-stripped with FSL's Brain Extraction Tool and high-pass–filtered at a 100-s cutoff.

Univariate fMRI analyses. Analysis of fMRI data were implemented in FSL v5.0.9 with FEAT (88), using the skull-stripped, temporally filtered, nonaggressively AROMA denoised data from FMRIPREP. For each experimental phase, subject-specific lower-level general linear models were created using task regressors for all CS types (CS^+_{Near}, CS^-_{Near}, CS^+_{Far}, CS^-_{Far}) split into early (1 to 5) and late (6 to 10) trials. For the fear-reinstatement phase, early trials were instead defined only as the first three trials to best capture the renewal of fear prior to reextinction (*Statistical Analyses*). US trials were also modeled for the acquisition and reinstatement phases. These regressors were convolved with a double-gamma hemodynamic response function. All lower-level models included cerebrospinal fluid, white-matter, differentiated signal variance, and framewise displacement confound regressors. Furthermore, any timepoints with a framewise displacement above 0.6 mm were censored in the model. Contrasts of interest were set at the lower-level, assessing $[(CS^+_{Near} > CS^-_{Near}) > (CS^+_{Far} > CS^-_{Far})]$ and $[(CS^+_{Far} > CS^-_{Far}) > (CS^+_{Near} > CS^-_{Near})]$ within early and late trials. Crucially, these contrasts subtract out nonreinforced CS^- avatars at each corresponding distance, thereby controlling for lower-level effects related generically to stimulus distance, size, or visual salience.

Functional connectivity analyses modeled psychophysiological interactions (PPI) between task conditions in a priori ROIs, including bilateral amygdala, bilateral dorsal (posterior) hippocampi, and vmPFC masks that have been used in previous fear-conditioning studies (66). These ROIs were chosen based on their relevance to fear learning and extinction (89), and the dorsal hippocampus specifically due to the involvement of this region in processing spatial contextual information (90, 91). The ROIs were defined anatomically from the Wake Forest University PickAtlas software (92). The amygdala was defined from the TD library of the Wake Forest University PickAtlas, the dorsal hippocampus was part of the AAL library hippocampus defined as posterior to $y = -24$ mm in Montreal Neurological Institute (MNI) space, and the vmPFC was defined as BA25 in the TD library, dilated by 2 mm. To investigate general changes in midbrain connectivity, we further defined a midbrain-PAG ROI following the same procedures detailed in other published work (93). Briefly, the Harvard–Oxford Subcortical Structural Atlas (94) was used to delineate the brainstem based on a 30% probability threshold, which was then further cropped at $z > -24$ mm and $y < -22$ mm in MNI space.

Higher-level group analyses for each phase employed FMRIB's local analysis of mixed effects – FLAME 1+2 (95). A single-group average (one-sample t test) design was used to determine the average response for each lower-level contrast. The cluster-forming threshold was set at $z = 2.3$, with a cluster significance threshold of $P = 0.05$. Contrast masking with $CS^+_{Near} > CS^-_{Near}$ or $CS^+_{Far} > CS^-_{Far}$ was used to ensure the appropriate directionality of the lower-level double subtractions. This application of FLAME 1+2 followed by cluster forming and significance threshold provides one of the most effective controls against the inflated false-positive findings that plague fMRI studies (96).

Multivariate RSA. For the RSA we were specifically interested in how neural representations present at the end of acquisition change throughout extinction learning, and whether this change is modulated by stimulus proximity. A dissimilarity metric (1 – Pearson correlation) was calculated between activity patterns within a predefined ROI in late acquisition and several time windows through extinction for each stimulus type for each participant, using voxel-wise t-statistic maps from the first-level analyses as input. This provided, for each time window for each participant, a metric of how dissimilar the neural patterns in the ROI were relative to the end of acquisition. We then investigated effects of CS type (CS^+/CS^- as well as Near/Far) on the behavior of these dissimilarity metrics throughout extinction.

The RSA was conducted in a region that displayed consistent activity for the $CS^+_{Near} > CS^-_{Near}$ contrast during both acquisition and extinction, right cerebellar lobule VI. The ROI was determined from a probabilistic cerebellar atlas provided within FSL (97, 98) and set at full probability to include all of right hemispheric lobule VI and extensions into vermal lobule VI. To further test the specificity of this result, we assessed bilateral amygdala, hippocampal, and vmPFC ROIs that were used in the PPI analyses. RSA analyses were performed in rsatoolbox (99) within the MATLAB programming environment, using contrast-of-parameter images for CS main effects generated from first-level FSL models set up similarly to those used in the univariate analyses. However, unlike the univariate analyses, these RSA first-level analyses used unsmoothed functional data that were not AROMA-denoised. Thus, to account for motion-related artifact, these models also specified head-motion parameters (rotation and translation) provided by FMRIPREP.

Dissimilarity was calculated between each pair of extinction trials and the last pair of acquisition trials. Although it is possible to extract similarity metrics from single trials, we averaged across every two trials in an attempt to reduce noise. We specifically compared extinction trials to the last two acquisition trials (as opposed to earlier in acquisition) in order to be more confident that the neural pattern was representative of a learned threat association. Similarly, we regressed dissimilarity metrics from the last two extinction trials with reinstatement shock-expectancy ratings in order to be more confident that the observed relationship was indicative of a maintained threat representation that had persisted throughout the entire extinction phase.

Statistical Analyses. SPSS Statistics 24 (IBM) was used for all statistical analyses of shock expectancy and skin conductance data. Trials were separated into CS^{+}_{Near}, CS^{-}_{Near}, CS^{+}_{Far}, CS^{-}_{Far} conditions and split into early and late trials based on presentation within each condition. Thus, each condition was separated into the first five and last five presentations of that character. Repeated-measures ANOVA was used to evaluate interactions of CS-Type (CS^{+} vs. CS^{-}), Distance (near vs. far), and Time (early vs. late). Since the reinstatement response is rather quick and temporary prior to reextinction, we instead focused analyses on only the first three trials for each condition, representing 30% of all of the trials, because the reinstatement phase delivered three shocks prior to any avatar presentations.

For the RSA analysis, we conducted a Time (E1 vs. E5) × Distance (Near vs. Far) repeated-measures ANOVA, followed by paired-sample *t* tests to determine if dissimilarity metrics changed from the first pair of extinction trials to the last pair of extinction trials. We further regressed dissimilarity metrics from the last pair of extinction trials with differential reinstatement shock-expectancy ratings ($CS^{+} > CS^{-}$) recorded on day 2. Regression plots with confidence bands were created in R.

Data Availability. The behavioral and psychophysiological data that support the findings of this study are available online in the Open Science Framework (100) at https://osf.io/jm62y/. Unthresholded statistical maps are available online in NeuroVault (101) at https://neurovault.org/collections/6221/.

ACKNOWLEDGMENTS. We thank Bao Doan for assistance with development of the virtual reality simulation in Unity. This work was supported by the National Science Foundation Graduate Research Fellowship Program (to L.F.) and National Science Foundation Grant BCS 1460909 (to K.S.L.).

1. D. Mobbs, C. C. Hagan, T. Dalgleish, B. Silston, C. Prévost, The ecology of human fear: Survival optimization and the nervous system. *Front. Neurosci.* **9**, 55 (2015).
2. M. S. Fanselow, The role of learning in threat imminence and defensive behaviors. *Curr. Opin. Behav. Sci.* **24**, 44–49 (2018).
3. J. E. LeDoux, Coming to terms with fear. *Proc. Natl. Acad. Sci. U.S.A.* **111**, 2871–2878 (2014).
4. D. Stjepanović, K. S. LaBar, "The cognitive neuroscience of fear learning" in *Stevens' Handbook of Experimental Psychology and Cognitive Neuroscience*, J. T. Wixted, Ed. (John Wiley & Sons, ed. 4, 2018), pp. 27–66.
5. J. LeDoux, The emotional brain, fear, and the amygdala. *Cell. Mol. Neurobiol.* **23**, 727–738 (2003).
6. K. S. LaBar, R. Cabeza, Cognitive neuroscience of emotional memory. *Nat. Rev. Neurosci.* **7**, 54–64 (2006).
7. T. F. Giustino, S. Maren, The role of the medial prefrontal cortex in the conditioning and extinction of fear. *Front. Behav. Neurosci.* **9**, 298 (2015).
8. A. Marschner, R. Kalisch, B. Vervliet, D. Vansteenwegen, C. Büchel, Dissociable roles for the hippocampus and the amygdala in human cued versus context fear conditioning. *J. Neurosci.* **28**, 9030–9036 (2008).
9. J. E. Dunsmoor, S. E. Prince, V. P. Murty, P. A. Kragel, K. S. LaBar, Neurobehavioral mechanisms of human fear generalization. *Neuroimage* **55**, 1878–1888 (2011).
10. S. Lissek *et al.*, Neural substrates of classically conditioned fear-generalization in humans: A parametric fMRI study. *Soc. Cogn. Affect. Neurosci.* **9**, 1134–1142 (2014).
11. L. Y. Maeng, M. R. Milad, Post-traumatic stress disorder: The relationship between the fear response and chronic stress. *Chronic Stress (Thousand Oaks)* **1**, 2470547017713297 (2017).
12. M. B. L. Careaga, C. E. N. Girardi, D. Suchecki, Understanding posttraumatic stress disorder through fear conditioning, extinction and reconsolidation. *Neurosci. Biobehav. Rev.* **71**, 48–57 (2016).
13. N. Reggente *et al.*, Enhancing the ecological validity of fMRI memory research using virtual reality. *Front. Neurosci.* **12**, 408 (2018).
14. J. M. Darves-Bornoz *et al.*; ESEMeD/MHEDEA 2000 Investigators, Main traumatic events in Europe: PTSD in the European study of the epidemiology of mental disorders survey. *J. Trauma. Stress* **21**, 455–462 (2008).
15. C. L. May, B. E. Wisco, Defining trauma: How level of exposure and proximity affect risk for posttraumatic stress disorder. *Psychol. Trauma* **8**, 233–240 (2016).
16. Ö. Frans, J. Åhs, E. Bihre, F. Åhs, Distance to threat and risk of acute and posttraumatic stress disorder following bank robbery: A longitudinal study. *Psychiatry Res.* **267**, 461–466 (2018).
17. M. S. Fanselow, L. S. Lester, "A functional behavioristic approach to aversively motivated behavior: Predatory imminence as a determinant of the topography of defensive behavior" in *Evolution and Learning*, R. C. Bolles, M. D. Beecher, Eds. (Lawrence Erlbaum Associates, 1988), pp. 185–212.
18. B. M. De Oca, J. P. DeCola, S. Maren, M. S. Fanselow, Distinct regions of the periaqueductal gray are involved in the acquisition and expression of defensive responses. *J. Neurosci.* **18**, 3426–3432 (1998).
19. L. R. Halladay, H. T. Blair, Distinct ensembles of medial prefrontal cortex neurons are activated by threatening stimuli that elicit excitation vs. inhibition of movement. *J. Neurophysiol.* **114**, 793–807 (2015).
20. S. Koutsikou, R. Apps, B. M. Lumb, Top down control of spinal sensorimotor circuits essential for survival. *J. Physiol.* **595**, 4151–4158 (2017).
21. T. C. Watson *et al.*, The olivo-cerebellar system and its relationship to survival circuits. *Front. Neural Circuits* **7**, 72 (2013).
22. O. K. Faull, K. T. S. Pattinson, The cortical connectivity of the periaqueductal gray and the conditioned response to the threat of breathlessness. *eLife* **6**, e21749 (2017).
23. P. Tovote *et al.*, Midbrain circuits for defensive behaviour. *Nature* **534**, 206–212 (2016).
24. E. J. Kim *et al.*, Dynamic coding of predatory information between the prelimbic cortex and lateral amygdala in foraging rats. *Sci. Adv.* **4**, r7328 (2018).
25. D. Mobbs *et al.*, When fear is near: Threat imminence elicits prefrontal-periaqueductal gray shifts in humans. *Science* **317**, 1079–1083 (2007).
26. D. Mobbs *et al.*, From threat to fear: The neural organization of defensive fear systems in humans. *J. Neurosci.* **29**, 12236–12243 (2009).
27. A. L. Gold, R. A. Morey, G. McCarthy, Amygdala-prefrontal cortex functional connectivity during threat-induced anxiety and goal distraction. *Biol. Psychiatry* **77**, 394–403 (2015).
28. D. Sun *et al.*, Threat-Induced anxiety during goal pursuit disrupts amygdala-prefrontal cortex connectivity in posttraumatic stress disorder. *Transl. Psychiatry* **10**, 61, 10.1038/s41398-020-0739-4 (2020).
29. J. Rosén, G. Kastrati, F. Åhs, Social, proximal and conditioned threat. *Neurobiol. Learn. Mem.* **142**, 236–243 (2017).
30. J. Rosén, G. Kastrati, A. Reppling, K. Bergkvist, F. Åhs, The effect of immersive virtual reality on proximal and conditioned threat. *Sci. Rep.* **9**, 17407 (2019).
31. F. Åhs, J. E. Dunsmoor, D. Zielinski, K. S. LaBar, Spatial proximity amplifies valence in emotional memory and defensive approach-avoidance. *Neuropsychologia* **70**, 476–485 (2015).
32. S. Qi *et al.*, How cognitive and reactive fear circuits optimize escape decisions in humans. *Proc. Natl. Acad. Sci. U.S.A.* **115**, 3186–3191 (2018).
33. D. Mobbs, The ethological deconstruction of fear(s). *Curr. Opin. Behav. Sci.* **24**, 32–37 (2018).
34. M. S. Fanselow, Z. T. Pennington, The danger of LeDoux and Pine's two-system framework for fear. *Am. J. Psychiatry* **174**, 1120–1121 (2017).
35. J. E. LeDoux, D. S. Pine, Using neuroscience to help understand fear and anxiety: A two-system framework. *Am. J. Psychiatry* **173**, 1083–1093 (2016).
36. D. Mobbs *et al.*, Viewpoints: Approaches to defining and investigating fear. *Nat. Neurosci.* **22**, 1205–1216 (2019).
37. T. Beckers, A. M. Krypotos, Y. Boddez, M. Effting, M. Kindt, What's wrong with fear conditioning? *Biol. Psychol.* **92**, 90–96 (2013).
38. S. Scheveneels, Y. Boddez, B. Vervliet, D. Hermans, The validity of laboratory-based treatment research: Bridging the gap between fear extinction and exposure treatment. *Behav. Res. Ther.* **86**, 87–94 (2016).
39. R. M. Visser, H. S. Scholte, T. Beemsterboer, M. Kindt, Neural pattern similarity predicts long-term fear memory. *Nat. Neurosci.* **16**, 388–390 (2013).
40. N. Omelchenko, S. R. Sesack, Periaqueductal gray afferents synapse onto dopamine and GABA neurons in the rat ventral tegmental area. *J. Neurosci. Res.* **88**, 981–991 (2010).
41. N. R. Ntamati, M. Creed, R. Achargui, C. Lüscher, Periaqueductal efferents to dopamine and GABA neurons of the VTA. *PLoS One* **13**, e0190297 (2018).
42. G. J. Kirouac, S. Li, G. Mabrouk, GABAergic projection from the ventral tegmental area and substantia nigra to the periaqueductal gray region and the dorsal raphe nucleus. *J. Comp. Neurol.* **469**, 170–184 (2004).
43. A. J. Beitz, The organization of afferent projections to the midbrain periaqueductal gray of the rat. *Neuroscience* **7**, 133–159 (1982).
44. K. D'Ardenne *et al.*, Role of prefrontal cortex and the midbrain dopamine system in working memory updating. *Proc. Natl. Acad. Sci. U.S.A.* **109**, 19900–19909 (2012).
45. M. Pignatelli *et al.*, Synaptic plasticity onto dopamine neurons shapes fear learning. *Neuron* **93**, 425–440 (2017).
46. A. E. Cavanna, M. R. Trimble, The precuneus: A review of its functional anatomy and behavioural correlates. *Brain* **129**, 564–583 (2006).
47. L. Frings *et al.*, Precuneus is involved in allocentric spatial location encoding and recognition. *Exp. Brain Res.* **173**, 661–672 (2006).
48. P. Nachev, C. Kennard, M. Husain, Functional role of the supplementary and pre-supplementary motor areas. *Nat. Rev. Neurosci.* **9**, 856–869 (2008).
49. M. A. Fullana *et al.*, Fear extinction in the human brain: A meta-analysis of fMRI studies in healthy participants. *Neurosci. Biobehav. Rev.* **88**, 16–25 (2018).
50. D. Hermans, M. G. Craske, S. Mineka, P. F. Lovibond, Extinction in human fear conditioning. *Biol. Psychiatry* **60**, 361–368 (2006).
51. M. A. Fullana *et al.*, Neural signatures of human fear conditioning: An updated and extended meta-analysis of fMRI studies. *Mol. Psychiatry* **21**, 500–508 (2016).
52. D. Mobbs *et al.*, Neural activity associated with monitoring the oscillating threat value of a tarantula. *Proc. Natl. Acad. Sci. U.S.A.* **107**, 20582–20586 (2010).

53. T. J. Albert, C. W. Dempesy, C. A. Sorenson, Anterior cerebellar vermal stimulation: Effect on behavior and basal forebrain neurochemistry in rat. *Biol. Psychiatry* **20**, 1267–1276 (1985).
54. M. Frings *et al*., Involvement of the human cerebellum in fear-conditioned potentiation of the acoustic startle response: A PET study. *Neuroreport* **13**, 1275–1278 (2002).
55. M. Maschke *et al*., Fear conditioned potentiation of the acoustic blink reflex in patients with cerebellar lesions. *J. Neurol. Neurosurg. Psychiatry* **68**, 358–364 (2000).
56. I. Lange *et al*., The anatomy of fear learning in the cerebellum: A systematic meta-analysis. *Neurosci. Biobehav. Rev.* **59**, 83–91 (2015).
57. B. Sacchetti, B. Scelfo, P. Strata, The cerebellum: Synaptic changes and fear conditioning. *Neuroscientist* **11**, 217–227 (2005).
58. B. G. Schreurs, P. A. Gusev, D. Tomsic, D. L. Alkon, T. Shi, Intracellular correlates of acquisition and long-term memory of classical conditioning in Purkinje cell dendrites in slices of rabbit cerebellar lobule HVI. *J. Neurosci.* **18**, 5498–5507 (1998).
59. B. Sacchetti, B. Scelfo, F. Tempia, P. Strata, Long-term synaptic changes induced in the cerebellar cortex by fear conditioning. *Neuron* **42**, 973–982 (2004).
60. A. Utz *et al*., Cerebellar vermis contributes to the extinction of conditioned fear. *Neurosci. Lett.* **604**, 173–177 (2015).
61. B. Sacchetti, T. Sacco, P. Strata, Reversible inactivation of amygdala and cerebellum but not perirhinal cortex impairs reactivated fear memories. *Eur. J. Neurosci.* **25**, 2875–2884 (2007).
62. J. Salmi *et al*., Cognitive and motor loops of the human cerebro-cerebellar system. *J. Cogn. Neurosci.* **22**, 2663–2676 (2010).
63. C. J. Stoodley, J. D. Schmahmann, Functional topography in the human cerebellum: A meta-analysis of neuroimaging studies. *Neuroimage* **44**, 489–501 (2009).
64. C. Habas *et al*., Distinct cerebellar contributions to intrinsic connectivity networks. *J. Neurosci.* **29**, 8586–8594 (2009).
65. O. Baumann, J. B. Mattingley, Functional topography of primary emotion processing in the human cerebellum. *Neuroimage* **61**, 805–811 (2012).
66. F. Åhs, P. A. Kragel, D. J. Zielinski, R. Brady, K. S. LaBar, Medial prefrontal pathways for the contextual regulation of extinguished fear in humans. *Neuroimage* **122**, 262–271 (2015).
67. D. P. Kennedy, J. Gläscher, J. M. Tyszka, R. Adolphs, Personal space regulation by the human amygdala. *Nat. Neurosci.* **12**, 1226–1227 (2009).
68. A. Olsson, E. A. Phelps, Social learning of fear. *Nat. Neurosci.* **10**, 1095–1102 (2007).
69. P. Hyland *et al*., Variation in post-traumatic response: The role of trauma type in predicting ICD-11 PTSD and CPTSD symptoms. *Soc. Psychiatry Psychiatr. Epidemiol.* **52**, 727–736 (2017).
70. D. H. Skuse, J. S. Morris, R. J. Dolan, Functional dissociation of amygdala-modulated arousal and cognitive appraisal, in Turner syndrome. *Brain* **128**, 2084–2096 (2005).
71. V. Taschereau-Dumouchel, M. Kawato, H. Lau, Multivoxel pattern analysis reveals dissociations between subjective fear and its physiological correlates. *Mol. Psychiatry*, 10.1038/s41380-019-0520-3 (2019).
72. S. R. Green, P. A. Kragel, M. E. Fecteau, K. S. LaBar, Development and validation of an unsupervised scoring system (Autonomate) for skin conductance response analysis. *Int. J. Psychophysiol.* **91**, 186–193 (2014).
73. J. E. Dunsmoor, S. R. Mitroff, K. S. LaBar, Generalization of conditioned fear along a dimension of increasing fear intensity. *Learn. Mem.* **16**, 460–469 (2009).
74. O. Esteban *et al*., fMRIPrep: a robust preprocessing pipeline for functional MRI. *Nat. Methods* **16**, 111–116 (2019).
75. O. Esteban *et al*., poldracklab/fmriprep: 1.3.1.post1. https:/doi.org/10.5281/ZENODO.2590805. Accessed 13 March 2019.
76. K. Gorgolewski *et al*., Nipype: A flexible, lightweight and extensible neuroimaging data processing framework in python. *Front. Neuroinform.* **5**, 13 (2011).
77. K. Gorgolewski *et al*., Nipype: A flexible, lightweight and extensible neuroimaging data processing framework in Python. 0.13.1 (2017). https://zenodo.org/record/581704#.XtpV9zpKhk4. Accessed 13 March, 2019.
78. N. J. Tustison *et al*., N4ITK: Improved N3 bias correction. *IEEE Trans. Med. Imaging* **29**, 1310–1320 (2010).
79. V. Fonov, C. Almli, A. Evans, D. Collins, R. McKinstry, Unbiased nonlinear average age-appropriate brain templates from birth to adulthood. *Neuroimage* **47**, S102 (2009).
80. B. B. Avants, C. L. Epstein, M. Grossman, J. C. Gee, Symmetric diffeomorphic image registration with cross-correlation: Evaluating automated labeling of elderly and neurodegenerative brain. *Med. Image Anal.* **12**, 26–41 (2008).
81. Y. Zhang, M. Brady, S. Smith, Segmentation of brain MR images through a hidden Markov random field model and the expectation-maximization algorithm. *IEEE Trans. Med. Imaging* **20**, 45–57 (2001).
82. R. W. Cox, AFNI: Software for analysis and visualization of functional magnetic resonance neuroimages. *Comput. Biomed. Res.* **29**, 162–173 (1996).
83. M. Jenkinson, P. Bannister, M. Brady, S. Smith, Improved optimization for the robust and accurate linear registration and motion correction of brain images. *Neuroimage* **17**, 825–841 (2002).
84. D. N. Greve, B. Fischl, Accurate and robust brain image alignment using boundary-based registration. *Neuroimage* **48**, 63–72 (2009).
85. J. D. Power *et al*., Methods to detect, characterize, and remove motion artifact in resting state fMRI. *Neuroimage* **84**, 320–341 (2014).
86. R. H. R. Pruim *et al*., ICA-AROMA: A robust ICA-based strategy for removing motion artifacts from fMRI data. *Neuroimage* **112**, 267–277 (2015).
87. A. Abraham *et al*., Machine learning for neuroimaging with scikit-learn. *Front. Neuroinform.* **8**, 14 (2014).
88. M. W. Woolrich, B. D. Ripley, M. Brady, S. M. Smith, Temporal autocorrelation in univariate linear modeling of FMRI data. *Neuroimage* **14**, 1370–1386 (2001).
89. S. Maren, Seeking a spotless mind: Extinction, deconsolidation, and erasure of fear memory. *Neuron* **70**, 830–845 (2011).
90. J. Ji, S. Maren, Electrolytic lesions of the dorsal hippocampus disrupt renewal of conditional fear after extinction. *Learn. Mem.* **12**, 270–276 (2005).
91. M. Zelikowsky, D. L. Pham, M. S. Fanselow, Temporal factors control hippocampal contributions to fear renewal after extinction. *Hippocampus* **22**, 1096–1106 (2012).
92. J. A. Maldjian, P. J. Laurienti, R. A. Kraft, J. H. Burdette, An automated method for neuroanatomic and cytoarchitectonic atlas-based interrogation of fMRI data sets. *Neuroimage* **19**, 1233–1239 (2003).
93. J. E. Smith, A. D. Lawrence, A. Diukova, R. G. Wise, P. J. Rogers, Storm in a coffee cup: Caffeine modifies brain activation to social signals of threat. *Soc. Cogn. Affect. Neurosci.* **7**, 831–840 (2012).
94. R. S. Desikan *et al*., An automated labeling system for subdividing the human cerebral cortex on MRI scans into gyral based regions of interest. *NeuroImage* **31**, 968–980 (2006).
95. M. W. Woolrich, T. E. J. Behrens, C. F. Beckmann, M. Jenkinson, S. M. Smith, Multilevel linear modelling for FMRI group analysis using Bayesian inference. *NeuroImage* **21**, 1732–1747 (2004).
96. A. Eklund, T. E. Nichols, H. Knutsson, Cluster failure: Why fMRI inferences for spatial extent have inflated false-positive rates. *Proc. Natl. Acad. Sci.* **113**, 7900–7905 (2016).
97. J. Diedrichsen, J. H. Balsters, J. Flavell, E. Cussans, N. Ramnani, A probabilistic MR atlas of the human cerebellum. *NeuroImage* **46**, 39–46 (2009).
98. J. Diedrichsen *et al*., Imaging the deep cerebellar nuclei: a probabilistic atlas and normalization procedure. *NeuroImage* **54**, 1786–1794 (2011).
99. H. Nili *et al*., A toolbox for representational similarity analysis. *PLoS Comput. Biol.* **10**, e1003553 (2014).
100. L. Faul *et al*, Proximal threats promote enhanced acquisition and persistence of reactive fear learning circuits. Open Science Framework. https://osf.io/jm62y. Deposited 17 June 2020.
101. L. Faul *et al*, Proximal threats promote enhanced acquisition and persistence of reactive fear learning circuits. NeuroVault. https://neurovault.org/collections/6221/. Deposited 16 December 2019.